



Comparison of mapping approaches of design annual maximum daily precipitation

J. Szolgay^{a,*}, J. Parajka^b, S. Kohnová^a, K. Hlavčová^a

^a Department of Land and Water Resources Management, Faculty of Civil Engineering, Slovak University of Technology, Radlinského 11, 813 68 Bratislava, Slovakia

^b Institute of Hydraulics, Hydrology and Water Resources Management, Vienna University of Technology, Karlsplatz 13/223, A-1040 Vienna, Austria

ARTICLE INFO

Article history:

Accepted 31 August 2008

Keywords:

Maximum daily precipitation totals
Design precipitation mapping
Regional frequency analysis
L-moments

ABSTRACT

In this study 2-year and 100-year annual maximum daily precipitation for rainfall–runoff studies and estimating flood hazard were mapped. The daily precipitation measurements at 23 climate stations from 1961–2000 were used in the upper Hron basin in central Slovakia. The choice of data preprocessing and interpolation methods was guided by their practical applicability and acceptance in the engineering hydrologic community. The main objective was to discuss the quality and properties of maps of design precipitation with a given return period with respect to the expectations of the end user. Four approaches to the preprocessing of annual maximum 24-hour precipitation data were used, and three interpolation methods employed. The first approach is the direct mapping of at-site estimates of distribution function quantiles; the second is the direct mapping of local estimates of the three parameters of the GEV distribution. In the third, the daily precipitation totals were interpolated into a regular grid network, and then the time series of the maximum daily precipitation totals in each grid point of the selected region were statistically analysed. In the fourth, the spatial distribution of the design precipitation was modeled by quantiles predicted by regional precipitation frequency analysis using the Hosking and Wallis procedure. The three interpolation methods used were the inverse distance weighting, nearest neighbor and the kriging method. Visual inspection and jackknife cross-validation were used to compare the combination of approaches.

© 2009 Elsevier B.V. All rights reserved.

1. Introduction

Recently, intensive efforts to develop complex statistical and spatial interpolation methods for estimating design rainfalls have been reported in the literature and also by several national authorities and meteorological offices of the world. As a result, hydrological maps of design and extreme precipitation have been produced for national hydrological atlases (e.g., in the USA (Bonnin, 2003); in Austria (HAÖ, 2003); in Germany (HAD, 2003); in Switzerland (HADES, 2004); and also the *Landscape Atlas of Slovakia* (2002). Printed or web-based engineering manuals have also been published. In Great Britain, the Flood Studies Report (FSR, 1975) and, subsequently, the Flood

Estimation Handbook (FEH, 1999) summarised methods of estimating extraordinary flood events, including procedures for estimating design precipitation. Other examples of complex national studies on heavy precipitation risk assessments include the German KOSTRA project (e.g., Stalman et al., 2004); the Italian VAPI project (Ferrari, 1994); the HIRDS system in New Zealand (Thompson, 2002); and the Australian Guide to Rainfall and Runoff (Pilgrim, 1987). In Slovakia, similar extreme precipitation event studies have been published by Šamaj et al. (1985), Faško et al. (2000), and Parajka et al. (2002, 2004), where in some cases, mapping of precipitation magnitudes for a given frequency also complemented the statistical analyses.

In this study we propose to compare a combination of four different approaches to the mapping of design annual maximum 24-hour precipitation totals and three interpolation methods. The daily precipitation measurements at 23 climate stations from 1961–2000 were used in the upper Hron basin in central Slovakia. The choice was directed toward simple robust

* Corresponding author.

E-mail addresses: jan.szolgay@stuba.sk (J. Szolgay), parajka@hydro.tuwien.ac.at (J. Parajka), silvia.kohnova@stuba.sk (S. Kohnová), kamila.hlavcova@stuba.sk (K. Hlavčová).

methods, which can find application in engineering hydrology studies. The three interpolation methods used were the inverse distance weighting, nearest neighbor and the kriging method.

The first method is the direct mapping of estimates of quantiles (2-year and 100-year values); the second is the direct mapping of the three parameters of local estimates of the GEV distribution. For the third method we have proposed a different approach, which to the best of our knowledge, has not yet been used for this purpose. First, the daily measurements of the precipitation totals were interpolated over a regular grid network in a catchment, and then the time series of the maximum daily precipitation totals in each grid point of the selected region were statistically analysed at site. As the advantage of the proposed algorithm in comparison to the direct mapping of design precipitation values it is considered that, if a physically adequate interpolation is used and adequate data is available, it enables the estimation of design values at ungauged sites for an interpolated time series. This may better reflect the physical and regional properties of the precipitation extremes as well as a description of the seasonal variations of the extreme daily precipitation totals over the selected region.

For the purpose of comparison, in the fourth method, the spatial distribution of the design precipitation was modeled by quantile values as predicted by a regional precipitation analysis. For this purpose the Hosking and Wallis (1997) procedure was adopted for mapping. The homogeneity of the region of interest was tested, and the dimensionless regional frequency distribution derived by using *L*-moments and the index value (the mean annual maximum daily precipitation) was mapped using spatial interpolation (instead of the more usual regional regression).

The paper is organized as follows. In the next section methods for extremes precipitation mapping are reviewed. Section 3 introduces the pilot region, describes the data used, presents the methods used in the data analysis and mapping, and discusses their applicability for the specific precipitation regime of the pilot region. The results of the mapping exercises and their comparison are presented in Section 4. Cross validation was used to compare the combination of approaches, which is followed by the discussion and concluding remarks.

2. Mapping of extreme precipitation for engineering design

The problem of mapping the spatial distribution of extreme precipitation involves a statistical description of the properties of extremes locally at-site (for a general overview, see, e.g., Katz et al., 2002) and a process of translating the point information registered at different climatic stations in a region in the form of a spatially continuous variable. In the first step the variables to be used to describe the spatial behavior of extreme precipitation are chosen (e.g., the median, the mean, various quantiles, distribution parameters or absolute maxima (García-Ruiz et al., 2000)). Next, the variables estimated locally are distributed using spatial interpolation techniques. Once the spatial models of the distribution parameters are known, various maps of the probabilities, quantiles, and return periods can be derived according to the needs of the user.

Spatial interpolation can be undertaken through the use of various algorithms. In climatological applications Thiessen polygons (Thiessen, 1911), the inverse square distance, the inverse distance weight, polynomial trend surfaces, partial thin

plate splines, trend surface analysis, the regularized spline with tension method (Mitášová and Mitáš, 1993), kriging methods without the use of an external variable (such as simple kriging, ordinary kriging, kriging with varying local means and block kriging) and kriging methods making use of a secondary variable (such as factorial kriging, kriging with an external drift and cokriging) (Carrera-Hernández and Gaskin, 2007; Pecušová et al., 2004) are used. In the spatial interpolation comparison exercises (e.g. Dubois, 1998) also other interpolation techniques have been applied such as linear and zone kriging, neural network residual kriging, multiquadratic functions and probability class kriging.

In extreme rainfall analysis, classic methodological approaches and recent advances in theory, both of the frequency analysis of extremes and spatial interpolation techniques, have found application as it will be illustrated on selected examples in the following short review. For example, the FEH method of estimating design rainfalls comprises two stages: mapping an index rainfall and deriving the rainfall growth curves. Growth curves, which relate the rainfall of various return periods to the index rainfall, have been derived by the FORGEX method, which is described by Reed et al. (1999). The mapping of the index rainfall across the UK was described by Faulkner and Prudhomme (1998) and Prudhomme (1999). The median annual maximum rainfall was selected as the index variable in the rainfall frequency analysis and kriging used to produce the final maps for the UK.

The HIRDS computer-based procedure for estimating design rainfalls in New Zealand was first developed in 1992 around established methods of rainfall frequency analysis (Thompson, 1992). The updated version (Thompson, 2002) involves a regional frequency analysis based on probability weighted moments (Hosking and Wallis, 1997); the Region of Influence regionalization method (Burn, 1990) and the mapping of an index rainfall (the median value of the annual maximum rainfall) and regional growth curves, respectively, by fitting a trivariate thin-plate spline to the longitude, latitude and site elevation.

The regionalization of extreme precipitation totals has attracted wide degree of interest in Switzerland in the preparation of the HADES atlas (HADES, 2004). Rainstorms were investigated by Geiger et al. (1986) and the spatial dependence of extreme rainfall parameters studied. This analysis resulted in the construction of several maps which permitted the estimation of design rainfall values up to duration of 5 days. In a follow-up study, Lang et al. (1998) studied 24-hour extreme point-precipitation values with a return period of 100 years and interpolated them for the whole area of the Swiss Alps. This allowed for the development of a map showing great spatial variations in the extreme precipitation statistics.

Rainfall frequency mapping for the whole territory of Greece was described in Loukas et al. (2001). Rainfall depths for durations of 1 to 7 days were fitted by the Extreme Value I (Gumbel) theoretical distribution and the depth-duration-frequency relationships for each station were estimated and mapped for Greece using spline interpolation.

Park et al. (2001) studied annual maxima of one and two day rainfalls over South Korea. The parameters of the Wakeby distribution were estimated at-site, and isoline maps of these estimates were presented. Weisse and Bois (2001, 2002) compared kriging and ordinary regression against topography to model 10 and 100-year rainfall estimates for rainfall

durations of 1–24 h in the French Alps concluding that topography is an important parameter for short time steps.

Within the KOSTRA project (e.g., Barthels et al., 1997; Stalman et al., 2004; Malitz, 2005), the regionalization of the N -year design rainfall values (for N ranging from 0.5 to 100 years) was achieved in two time frames using classical extreme value statistics and by means of a complex climatological analysis, including analyses of the altitudinal dependence of the circulation patterns and of geostatistical methods with a grid resolution of 8.5 km×8.5 km for the whole territory of Germany.

For the Landscape Atlas of Slovakia, Šamaj et al. (1985) and Faško et al. (2000) estimated the design rainfall for different return periods and hand drew isoline maps over the entire region of Slovakia supported by subjective reasoning. In Parajka et al. (2002, 2004), annual and seasonal maximum daily precipitation depths were used and contour and grid maps of the mean value, standard deviation, 100- and 2-year maximum annual and seasonal daily precipitation depths were derived using various interpolation methods such as Thiessen polygons, kriging, cokriging and the inverse weighting distance method.

Bonnin (2003) reported on the use of a regional L -moments frequency analysis technique, a spatial interpolation-based mapping procedure using a statistical-geographic approach, and a web-based delivery of the final product in the US.

Watkins et al. (2005) conducted regional precipitation frequency analyses and spatially interpolated point intensity duration frequency (IDF) estimates at gauged sites for Michigan. Several interpolation and smoothing techniques were evaluated including a trend surface analysis, thin plate splines, inverse distance weighting, and several kriging algorithms.

Beguiria and Vicente-Serrano (2006) described a procedure based on an extreme value analysis and spatial interpolation techniques assuming a probability model in which the extreme rainfall probability distribution function parameters vary smoothly in space. The at-site parameter

estimates (location, scale, and shape) were regressed upon a set of location and relief variables, which enabled the construction of a spatially explicit probability model.

Casas et al. (2007) studied maximum daily precipitation in Catalonia for several established return periods with a high spatial resolution. The maximum daily precipitation corresponding to return periods between 2 and 500 years were spatially analysed by applying the Cressman (1959) method.

Wallis et al. (2007) updated the precipitation–frequency atlas published by the US National Weather Service in 1973 using the PRISM mapping system and the regional L -moments algorithm for precipitation magnitude–frequency estimates for estimating 2-hour and 24 hour precipitation frequencies.

Cooley et al. (2007) presented a method for producing maps of precipitation return levels and uncertainty measures in the Colorado region. Separate hierarchical models were constructed for the intensity and frequency of extreme precipitation events. Geographical covariates such as elevation or mean annual precipitation were taken into account to yield parameter and return-level estimates which have a more spatial consistency.

The evaluation of frequency analysis and mapping methods with respect to climatological variables in general has been also addressed in Tabios and Salas (1985), Borge and Vizzacaro (1997), Dubois (1998), Goovaerts (2000), Jarvis and Stuart (2001), Weisse and Bois (2001), Brown and Comrie (2002), Hofierka et al. (2002), Lloyd (2005), Watkins et al. (2005), Carrera-Hernández and Gaskin (2007), and Daly (2006). From these it can also be seen that the choice of methods for both parts of the analysis is extremely rich. While the use of extreme value theory and especially the application of the L -moment method with the GEV distribution has become more or less a standard in hydrology for the statistical frequency analysis, the recommendations on the choice of spatial interpolation method were not so obvious. Many aspects can be taken into consideration, ranging from the field of application of the resulting map through the constraints imposed by the data availability, the time and the available resources to the selection of a physically adequate model for the given settings. Among



Fig. 1. Location of the upper Hron River basin in Slovakia.

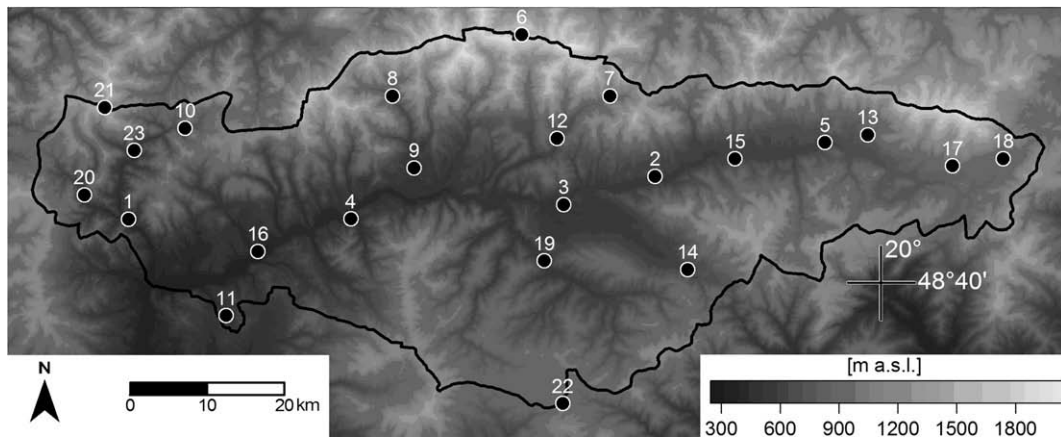


Fig. 2. Topography of the upper Hron River basin with the location of the climate stations.

these, consideration of the secondary variables seems to be the most important. A detailed review of the possibilities is beyond the scope of this study (for discussions on the topic see, e.g., Wolfson, 1975; Asli and Marcotte, 1995; Faulkner and Prudhomme, 1998; Wotling et al., 2000; Goovaerts, 2000). In conclusion, these studies did not provide a clear answer as to whether the use secondary variables always improves the spatial interpolation of daily rainfall. Some authors opine that although the use of elevation as an auxiliary variable improves the spatial interpolation of monthly rainfall data, the relationship between rainfall and elevation is less useful when interpolating daily data (Carrera-Hernández and Gaskin, 2007). On the other hand, assimilation of other climatic variables, including those from weather models, seems to improve mapping performance.

3. Data and methods

3.1. Study area

In this study the upper Hron River basin with an area of 1766 km² was selected as a pilot area. The Hron River basin is located in central Slovakia, and it was chosen as representative of mountainous regions in Slovakia (Fig. 1). The minimum elevation of the basin is 340 m a.s.l.; the maximum elevation is 2004 m a.s.l.; and the mean elevation is 850 m a.s.l. 70% of the basin area is covered by forest, 10% by grasslands, 17% by agricultural land and 3% by urban areas. The digital elevation model of the basin and the location of the climatic stations used in this study are in Fig. 2.

The climate conditions of the upper Hron River basin are summarised in Table 1 for the valleys and mountainous slopes of the region separately. The mean annual precipitation within the study area decreases from the western slopes of the Starohorske Mountains (1000 mm), to the Hron River Valley (700 mm) and increases again up to 1800 mm, at the highest elevation of the Low Tatras. The mean temperature in winter season varies from -4.0 °C to -5.5 °C in the valleys, and is about -9 °C on the mountainous slopes. In summer months the average value of observed temperature is 7 to 18 °C. The mean actual evaporation in the region varies from 200–450 mm.

3.2. Precipitation data

In the study the annual maximum 24-hour precipitation totals are analysed, which is the greatest amount of precipitation in a 12-month period for a 24-hour duration measured from 6 am to 6 am of the next day and associated with the date of the previous day. The calendar year was used for determining precipitation annual maxima for 24 h in this study, and the data was obtained from the precipitation records of the Slovak Hydrometeorological Institute.

The selection of climatic stations aimed at covering the whole region uniformly with stations which have a complete series (without missing data) of observations during the period 1961–2000. The final dataset included 23 climatic stations; their spatial distribution is shown in Fig. 2. The elevation histogram in Fig. 3 shows the altitudinal distribution of the stations together with the percentage of the basin area belonging to the respective elevation zones. It can be seen, that the two empirical distributions show similar densities, and that the stations are mainly located in the range of the elevation of 300 up to 1200 m a.s.l. with the majority of them being placed at elevations below 800 m a.s.l. This fact is typical for the altitudinal distribution of stations in Central Europe, where higher elevations are not adequately covered by the data and it complicates both climatological and hydrologic analyses and therefore has to be taken into consideration when selecting methods and interpreting results.

Table 1
Values of selected climatic characteristics of the upper Hron River basin.

Climate characteristics	Valleys	Mountainous slopes
Mean air temperature [°C] – January	(-4.0)–(-5.5)	(-4.5)–(-9.0)
Mean air temperature [°C] – July	18.0–14.5	15.0–7.0
Mean annual precipitation [mm]	600–850	700–1500
Mean annual precipitation in warm season (April–September) [mm]	350–550	400–800
Mean annual precipitation in cold season (October–March) [mm]	300–400	300–700
Mean annual evaporation [mm]	400–450	450–200

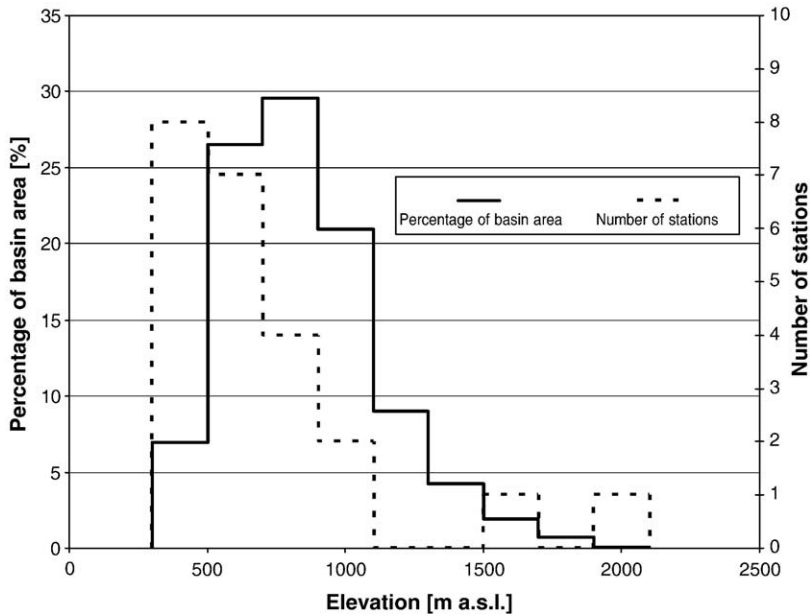


Fig. 3. Basin area elevation zones and the histogram of altitudinal distribution of the climate stations in the upper Hron River basin used in this study (the full line shows the distribution of elevations, the dashed line the distribution of precipitation stations).

3.3. Extreme precipitation regime

In general, synoptic-scale cyclonic weather systems and associated atmospheric fronts generally provide a mechanism for producing annual maxima of precipitation in the region. Precipitation can be enhanced in mountainous areas as atmospheric moisture is lifted over the Low Tatras or the Slovenske Rudohorie.

The synoptic analysis by Lapin et al. (2002) showed that in the upper Hron River region the synoptic situations of type B (a slowly progressing low-pressure trough with an axis over Central Europe), type C (a slowly progressing cyclone with a center over Central Europe) and type Bp (a low-pressure trough with an axis over Central Europe moving from the west to the east) predominantly influence extreme precipitation events with a cyclonic origin. During these synoptic situations, in general, relatively very warm air masses with high humidity flow from the southwest to the east over the Hron River basin. These types of synoptic situations caused about 60–65% cases of maximum precipitation depths with a duration of 2 or more days in the region during the period of 1951–2000.

Annual maximum precipitation with a 24-hour duration occurs predominately in the summer months as a result of several storm generating mechanisms. They may occur due to convective activity associated with synoptic weather systems. In such a case, the 24-hour annual maxima are embedded within rains of a longer duration. They may also occur due to intense convective activity not associated with an organised weather system but with thunderstorms in late spring, summer and early autumn. These are of shorter duration than one day, occur mainly in the late afternoon, and have limited areal coverage. The mean annual number of thunderstorm days is about 30 in the upper Hron River basin; some stations can also have more than 35 days on average. The number of thunderstorm days does not show altitudinal dependence.

Fig. 4 shows the percentage of the occurrence of annual basin average maximum 1–5 day precipitation totals in individual months from 1961–2000 in the upper Hron River basin to Banska Bystrica. It can be seen that most of the heavy precipitation events in summer season occur from June to

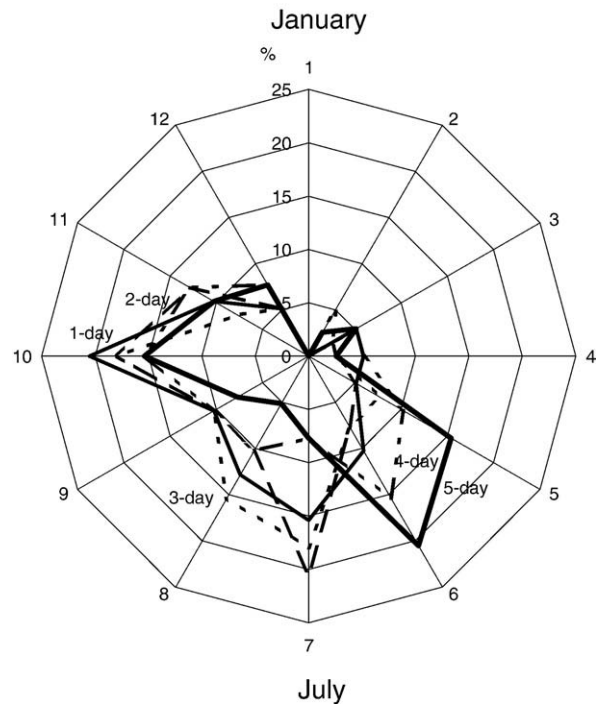


Fig. 4. Percentage of the occurrence of annual basin average maximum 1–5 day precipitation totals in individual months (from January (month 1) to December (month 12)) from 1961–2000 in the upper Hron River basin to Banska Bystrica.

September. In the cold season, the majority of the precipitation events are observed during the months of October to December. There are very rare situations with extreme precipitation events in January and March.

The seasonality analysis of 24-hour annual maximum precipitation was done based on an estimation of the seasonality index of the annual maximum daily precipitation totals according to Burn (1997), which indicates the distribution of extreme precipitation occurrences within a year and indirectly proves that these are due to convective events without the need of analyzing each event individually.

Burn's vector (Burn, 1997) represents the variability of the date of occurrence of an extreme event; in particular, its direction is the mean date of the occurrence of the extreme event and the modulus is the variability around the mean value. Considering the date of the occurrence of the extreme event as a Julian date, where January 1 is the 1st day and December 31 is the 365th day, and converting it into an angle in radians, one gets

$$\theta_i = J_i \frac{360^\circ}{365.25}, \quad \theta_i \in \{0, 98^\circ, \dots, 360^\circ\}. \quad (1)$$

Thus, the date of an extreme event can be interpreted as a vector with a unit magnitude and direction θ_i . The mean direction of an n -event sample is given as

$$\bar{\theta} = \arctg\left(\frac{\bar{y}}{\bar{x}}\right), \quad \bar{\theta} \in (0^\circ; 360^\circ), \quad (2)$$

where $\bar{\theta}$ is in radians and

$$\bar{x} = \frac{1}{n} \sum_{i=1}^n \cos\theta_i, \quad \bar{y} = \frac{1}{n} \sum_{i=1}^n \sin\theta_i. \quad (3)$$

The variability around the mean value is obtained by calculating the modulus of the average vector, defined as the seasonal concentration index:

$$\bar{r} = \sqrt{\bar{x}^2 + \bar{y}^2}, \quad \bar{r} \in (0; 1). \quad (4)$$

This assumes values between 0 and 1. For $\bar{r} \rightarrow 0$, there is no single dominant season, and the time of the occurrence of an extreme event is distributed around the year; for $\bar{r} = 1$ the extreme events occur on the same day. Thus the larger values indicate a greater regularity in the time of an occurrence. The couple $(\bar{\theta}, \bar{r})$ defines the Burn's vector.

The results in Fig. 5 show the values of the seasonal concentration index \bar{r} in a range of 0.4–0.8 and the prevailing occurrence of extreme daily precipitation events in the months of July, August and September, which is represented by the angle for 56 stations from the whole Slovakia including the region of interest. These results are in accordance with the seasonality of maximum annual floods in the region regardless of the basin size (Hlavčová et al., 2005).

3.4. Frequency analysis of annual maximum 24-hour precipitation

The steps in traditional design precipitation estimation are as follows:

1. Choose an appropriate distribution on the basis of some criterion.

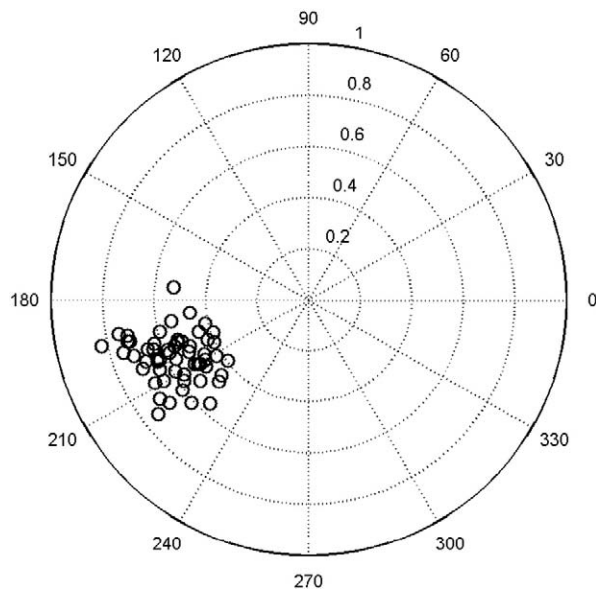


Fig. 5. Location of seasonal concentration index \bar{r} for maximum daily precipitation totals in Slovakia. The angles represent: 0° – January 1st, 90° – April 1st, 180° – July 1st and 270° – October 1st.

2. Estimate the parameters of this distribution.
3. Determine the design value with a selected return period. For annual maximum values it holds that the given exceedance probability is $q = 1/T$, where T is the return period.

Two underlying assumptions of frequency analysis which should be tested are the stationarity and independence of the data at a given site. Here, standard statistical tests for stationarity and serial independence of annual maximum daily precipitation were conducted. Stationarity can be assessed through trend analysis; the data must be free from trends during the observation period. This was confirmed for each station by standard linear regression techniques and the difference-sign test (Cipra, 1986) was used to test for significant trends. The test values were close to zero, the maximum value reached was 0.8 which was below the critical value of 1.9. The null hypothesis could not be rejected at the 5% level, so the data was accepted as stationary. Stationarity of flood series at the Hron River basin which were tested in Pekárová and Pekár (2004) showed similar results.

In order to confirm the independence of the annual maxima data, autocorrelation coefficients were computed for the data at each gauge. All the autocorrelation coefficients achieved lower values than 0.3 and were tested against a null hypothesis of zero serial correlation (independence). The null hypothesis could not be rejected at the 5% level so, as expected, the annual maxima data were found to be serially independent.

Unfortunately, our prior knowledge of hydrometeorological processes is not sufficient for the choice of an appropriate theoretical distribution. The extreme value theory can be of help in a broader sense since the data itself may not provide a straightforward answer to the question of which theoretical distribution is the best one for a specific problem (Cunnane, 1985). As can be seen from the short review in the introduction, similar studies have also favored the use of such distributions,

e.g., the EV1 – Gumbel distribution, or GEV – General extreme value distribution (Geiger et al., 1986; Lang et al., 1998; Loukas et al., 2001; Casas et al., 2007; Wallis et al., 2007). The GEV is to be generally considered a suitable distribution (Hosking and Wallis, 1997) and therefore in the present study it was selected to be tested as a candidate both for at-site and a regional frequency analysis.

As for the parameter estimation methods, the maximum likelihood method is considered to be one that offers estimates that are superior from a statistical point of view (see, e.g., Kite, 1977). The method of *L*-moments is at present becoming the most popular method in hydrology since the parameter estimates are more robust for outliers in the data (Hosking, 1990; Vogel and Fennessey, 1993; Gottschalk and Krasovskaia, 2002). Therefore, the choice of an appropriate theoretical distribution and its parameter estimation was approached here through the method of *L*-moments. The same choice was also made in, e.g., Bonnín (2003), Wallis et al. (2007).

In order to increase the information content in the data, it is recommended to merge observations from the individual observation points (Hosking and Wallis, 1997) which come from a homogeneous region and to analyse not just individual series but to use also regional data. Homogeneity implies that a scaled data series has the same theoretical distribution. Clearly it seems unreasonable to believe that such an assumption would ever be entirely true. However, if only limited records are available at the sites in question, this is a reasonable approximation to make (Stedinger, 1983).

The method adopted here is based on the so-called index flood method, which was developed by Dalrymple (1960) and put into a new theoretical framework by Hosking and Wallis (1997), which has the following steps:

1. Scaling of each observation series by means of a parameter of the central tendency (mean, median, mode) – the so called index flood – here, the mean is used.
2. Estimation of the representative quantiles across the scaled regional sample and establishing the form of the distribution function and its parameters on the basis of the total regional data sample.

The time series of annual maximum daily precipitation totals in each station was analysed using *L*-moment statistics. The three parameters of the GEV distribution were estimated, the appropriateness of using the GEV distribution was tested in each station; and the 2-year and 100-year values of the annual maximum 24-hour precipitation were computed.

The identification and formation of homogeneous regions is an iterative process. Here it was anticipated that the Hron region would not require sub-division to meet the homogeneity criteria based also on results from Gaál (2006), who performed a regional frequency analysis for 56 precipitation stations covering the whole territory of Slovakia, also including stations from the upper Hron River basin. The convective characters of the 24-hour annual maximum precipitation and its weak altitudinal dependence also supports this decision, which was tested by the Hosking and Wallis (1997) homogeneity test. They proposed to test the homogeneity of pooled sites by a measure based on *L*-moment ratios, which compares the between-site variation in sample *L*-Cv (coefficient of a variation) values with the expected variation for a homogeneous pooling group. According to the *L*-moments used in the definition of the test

Table 2

Results of the Hosking–Wallis heterogeneity test.

Heterogeneity measure	Value of heterogeneity measure	Degree of homogeneity
H_1	– 1.94	Acceptably homogeneous
H_2	– 1.44	Acceptably homogeneous
H_3	– 1.62	Acceptably homogeneous

statistics (H_i), Hosking and Wallis defined three heterogeneity measures: H_1 – when *L*-Cv is used, H_2 – if the *L*-Cs is used and H_3 – if the *L*-Ck is applied. H_i values of the test for the upper Hron region are presented in Table 2.

Pooling groups are usually classified as acceptably homogeneous if $H_i < 1$ ($i = 1, 2, 3$), possibly homogeneous ($1 \leq H_i \leq 2$) and heterogeneous ($H_i > 2$). In the case of additional variability in the data H_1 less than 2 may be accepted as homogeneous for 24-hour precipitation (Wallis et al., 2007). According to the test, the whole region was found to be acceptably homogeneous. The negative values of H_i indicate, that there may be less dispersion among the at-site samples *L*-Cv values than would be expected of a homogenous region with independent at-site frequency distributions.

One of the primary tasks in the regional analyses was to identify the best probability distribution for describing the behavior of the annual maxima data. Plots of the regional *L*-Skewness and *L*-Kurtosis values for the Hron region with a 24-hour duration are shown in Fig. 6. In order to select the appropriate regional frequency distribution function for a particular pooling group, an *L*-moment ratio diagram was used. The *L*-moment ratio diagram is a widely used tool for the graphic interpretation and comparison of the sample *L*-moment ratios, *L*-Cs (skewness), and *L*-Ck (kurtosis) of various probability distributions (Hosking, 1990). The closeness of the regional mean and the at-site data to the GEV distribution is clearly evident.

Accordingly, a goodness-of-fit test statistic (Hosking and Wallis, 1997, 1993) was used in identifying the best three-parameter distribution. The goodness-of-fit test described by Hosking and Wallis (1997) is based on a comparison between the *L*-Ck sample and *L*-Ck population for different distributions. An acceptable distribution function should achieve a value of $|Z^{\text{DIST}}| \leq 1.64$ (for details see Hosking and Wallis, 1997). The results of the Z^{DIST} goodness-of-fit measure presented in Table 3 show three accepted distribution functions – General Logistic, General Extreme Value (GEV) and General Normal. The lowest value of Z^{DIST} was achieved by the GEV distribution.

Due to the location of the regional *L*-moment ratios (see Fig. 6) and also to the results of the test, the GEV distribution function was selected as the regional one, Table 4 contains the values of the quantiles of dimensionless regional frequency distribution function GEV.

3.5. The selection of the interpolation methods

The inverse distance weighting interpolation (IDW) method is first applied here, since it is a simple but efficient interpolation method which is often used in engineering applications. The IDW assigns weights to the neighboring observed values based on the distance to the interpolation

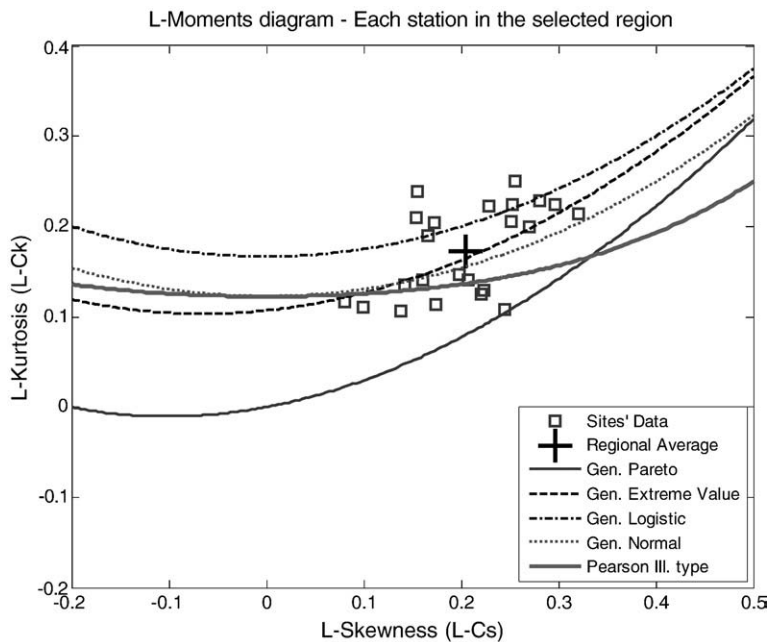


Fig. 6. L-moment ratio diagram for the precipitation stations in the upper Hron River region; the regional average is marked as a black cross.

location, and the interpolated value is the weighted average of the observations. IDW is applied in many precipitation mapping methods (e.g., Ahrens, 2006) and is sometimes combined with the declustering and directional grouping of stations or empirical adjustments with respect to orography (Daly, 2006). The standard IDW applies a geographical distance measure; Ahrens (2006) replaced it with some statistical distance measures. Here geographical distance was used.

The general form of the equation for interpolation in the (x,y) plane at point z_i (Meijerink et al., 1994) is:

$$z_0 = \sum_{i=1}^n w_i z_i, \tag{5}$$

where:

- z_0 is the estimated value of the process at any point x_0 and y_0 ,
- w_i is the weight of the sampling point i ,
- $z_i(x_i,y_i)$ is the observed value of the attribute at point x_i,y_i ,
- n is the number of sampling points considered.

The weights w_i are determined to be inversely proportional to a power of the distance between the interpolated point x_0, y_0 and the points with measurements x_i, y_i (for

details see e.g. Tabios and Salas, 1985). For this study the power parameter was set to be equal to two. This method is often used in engineering application, since it is simple and efficient. As it was established by Bloeschl and Grayson (2001), the IDW generates spurious artefacts in the case of highly variable quantities and irregularly spaced data sites.

If only the next neighbor is considered, the IDW method collapses to the next neighbor or the Thiessen method (Thiessen, 1911). This method is frequently used in hydrology for the spatial variability of the precipitation and will also be used here for purposes of comparison.

It can be shown that statistical interpolation methods like multiple linear regression, optimal interpolation or kriging can perform better than IDW, but only if the data's density is sufficient (Ahrens, 2006). Here the ordinary kriging was applied. It is a stochastic interpolation approach, which is designed to give the best linear unbiased estimate (B.L.U.E) of the variable of interest. The best means that the weights w_i are assessed by minimizing the variance of the interpolation error using a statistical relationship (spatial autocorrelation) between values at sampled points. The term linear means that the estimation of mapped variable in ungauged sites is based on a weighted linear combination of observations in neighborhood and the term unbiased refers to the zero bias of interpolation errors. More detailed description of the

Table 3 Results of the Z^{DIST} goodness-of-fit measure.

Type of distribution function	Z^{DIST} value
General logistic	1.60
General extreme value	-0.84
General normal	-1.44
Pearson type III	-2.68
General Pareto	-6.45

Table 4 Values of the quantiles of dimensionless GEV regional flood frequency distribution function.

Probability of exceedance	0.900	0.800	0.500	0.200	0.100	0.050	0.020	0.010
Quantile estimates	0.673	0.751	0.941	1.210	1.397	1.584	1.837	2.034

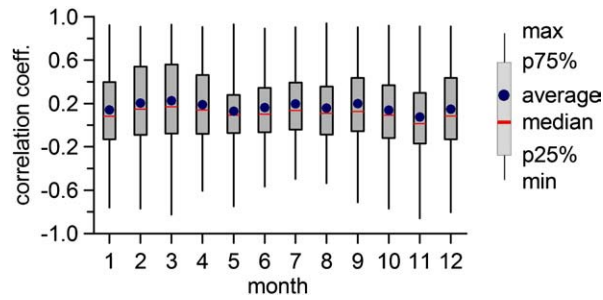


Fig. 7. Distribution of correlation coefficient between daily precipitation totals and elevation in each month.

algorithm is available in geostatistical literature (e.g. in Isaaks and Srivastava, 1989).

In order to support the choice of interpolation methods compared in this study, the relationship between an elevation and the mapped variables was also investigated.

First, the relationship between the daily precipitation totals and the catchment elevation was tested on each day in the period 1961–2000. As expected and as also reported in the climatological studies (e.g. Lapin et al., 2002) and due to the convective character of the 24-hour annual maximum precipitation in the region, the correlation was not significant in general and did not exhibit a uniform tendency – both positive and negative correlations were observed. This is illustrated in Fig. 7, where the monthly distribution of the correlation coefficients between the daily precipitation totals and the elevation are presented. The distributions are nearly symmetrical with the mean values of the correlation coefficients being low and oscillating around a value of 0.2.

Next, the 2-year and 100-year annual maximum 24-hour precipitation values were plotted against the station elevation; these plots are shown in Fig. 8. The associated R^2 coefficients are 0.001 and 0.02 respectively.

Fig. 9 shows the relationship between the at-site estimation of the GEV distribution and the station elevation. It can be seen that the dependence is insignificant, which is supported by the values of the correlation coefficients, which are 0.001, 0.11, 0.111, respectively for location, scale and the shape parameter of the GEV distribution.

Next, the 2-year and 100-year annual maximum 24-hour precipitation values were plotted against the station elevation for the case, in which the region was further divided into sub-regions. The division is knowledge-based and reflects the

general pattern of the precipitation regime as usually considered by climatologists. According to it, the upper Hron River basin could be divided into four sub-regions. In this case even the homogeneity analysis enabled the consideration of these sub-regions as homogeneous (see Table 5).

In only one of the sub-regions relationship of the mean annual maximum 24-hour precipitation with elevation could be expected (see Fig. 10). This sub-region is located at leeward sites in the eastern part of the basin (represented by the stations 5, 13, 15, 17 and 18). This region is open only for seldom occurring north-western atmospheric circulations. The rain shadow effect is caused here by the Low Tatras from the north and the Slovenské Rudohorie Mountains from the south. The others behave like in the previous analysis; as a consequence of this the elevation was not considered here as a secondary variable.

3.6. Assessing errors in spatial interpolation comparisons

In practice, the interpolated climate field is unknown, except at a relatively small number of observed points. The interpolation methods themselves do not provide useful internal estimates of error, because these rely on the very same assumptions used in the interpolation process itself (Daly, 2006).

An error statistic often reported in climate interpolation studies is the cross-validation error in jackknife cross-validation (Daly, 2006). This will be used in the present study. It measures the difference between a station's value and the model's estimate for that station, when the station has not been considered in the data set. Usually the removal of the station and an estimation of the error in its place are

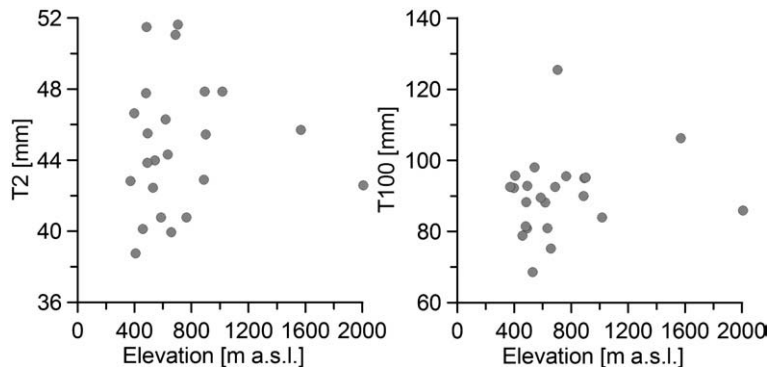


Fig. 8. Relationship between the estimated design 2-year and 100-year daily maximum precipitation totals calculated at the stations and the elevations.

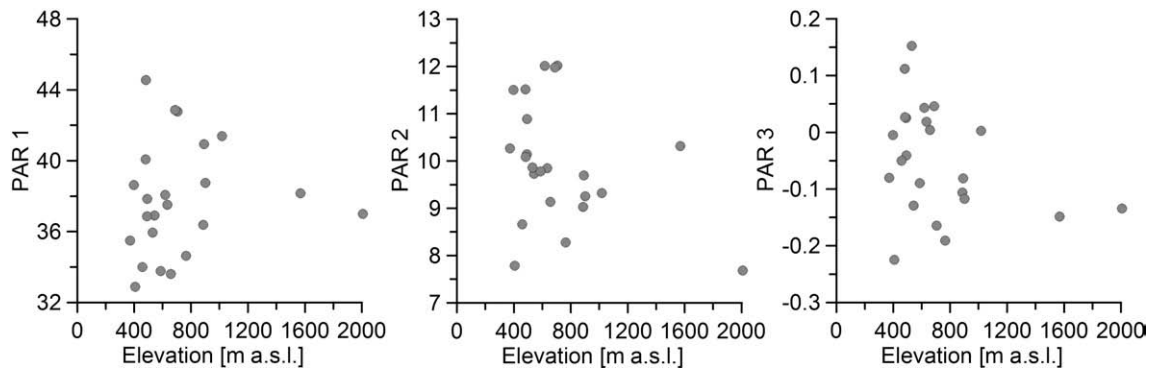


Fig. 9. Relationship between the parameters of the General Extreme Value distribution and elevation, where PAR1 – is the location parameter, PAR2 – the scale parameter and PAR3 – the shape parameter.

performed for each station one at a time, with the station returned to the data set after the estimation. Several overall error statistics, such as mean absolute error (MAE), bias, and others are calculated afterwards.

The method is relatively simple but also has several drawbacks. No error information is provided for places where there are no stations, and it has the tendency to underestimate errors when stations are located in pairs or clusters, since a nearby station can produce a good estimate for one that has been omitted from the data set during the jackknife deletion process (Daly, 2006).

4. Results

In this section different mapping approaches to the mapping of design annual maximum daily precipitation totals as well as different interpolation methods are compared and discussed. The first method is the direct mapping of at-site estimates of 2 and 100-year maximum daily precipitation totals. The second method is based on the direct mapping of at-site estimates of the three parameters of the GEV distribution. The third method is based on the interpolation of daily precipitation totals over a regular grid network in a catchment. In this method, the design annual maximum daily precipitation totals were estimated from the time series of the annual maximum daily precipitation totals in each grid point of the selected region. In the fourth method, the spatial distribution of the design precipitation was modelled by quantile values as predicted by a regional precipitation analysis. For this purpose the Hosking and Wallis procedure was adopted and the dimensionless regional frequency distribution derived by using L -moments and the index value (the mean annual maximum daily precipitation) was mapped using spatial interpolation.

Table 5

Values of the Hosking–Wallis heterogeneity test (H_i) for the selected sub-regions.

Number of the sub-region	H_1	H_2	H_3
1	–1.52	–1.53	–1.28
2	–0.9	–0.9	–0.28
3	–0.54	–0.1	–0.014
4	–1.45	–1.49	–1.25

The three interpolation methods used were the inverse distance weighting (IDW), nearest neighbor (nn) and the kriging method. Comparison of the mapping approaches and different interpolation methods was done using the jack-knife cross-validation procedure.

The results of the different approaches to mapping the design annual maximum daily precipitation totals are illustrated in Figs. 11a–c and 12a–c. In Fig. 11a–c, maps of the 2-year maximum daily precipitation totals, and in Fig. 12a–c, maps of the 100-year maximum daily precipitation totals are presented. In the figures the mapping approaches compared are labeled for the inverse distance weighting (a) and the kriging interpolation method (c) as follows: A = at site, B = interpolation of GEV moments, C = interpolation of daily precipitation to grids, D = regional interpolation according to Hosking and Wallis. For the nearest neighbor method (b) the first three mapping approaches produce identical maps and are labeled as A and the map by the regional frequency method is labeled as B.

In Fig. 11a–c similar spatial patterns in the maps of 2-years maximum daily precipitation totals obtained by different mapping approaches can be observed, with the exception of the approach based on the nearest neighbor interpolation. The spatial patterns introduced by this interpolation method for tested mapping approaches are very simple and should obviously be used only in case of sparse data.

Regardless of a low correlation between annual maximum daily precipitation totals, as well as between their design values with elevation, local effects of the terrain represented by orography are apparent in spatial patterns produced by the other interpolation methods. The lowest values of the design annual maximum daily precipitation totals in maps A, B and D are evident in the pattern of stations 5, 13 and 15 and around station 4; the highest values occurred in the pattern of stations 1, 10, 20, 21 and 23. These facts follow from the rain shadow effect for the leeward sites of stations 5, 13 and 15 and the increasing effect of the maximum daily precipitation on windward slopes for the pattern of stations 1, 10, 20, 21, and 23.

In map C, the design annual maximum daily precipitation totals are generally lower in comparison with the previous maps. There are usually higher values of the design annual maximum daily precipitation totals at the station sites than in neighboring grids. These results are caused by the smoothing effect of interpolations for daily precipitation totals, especially in the

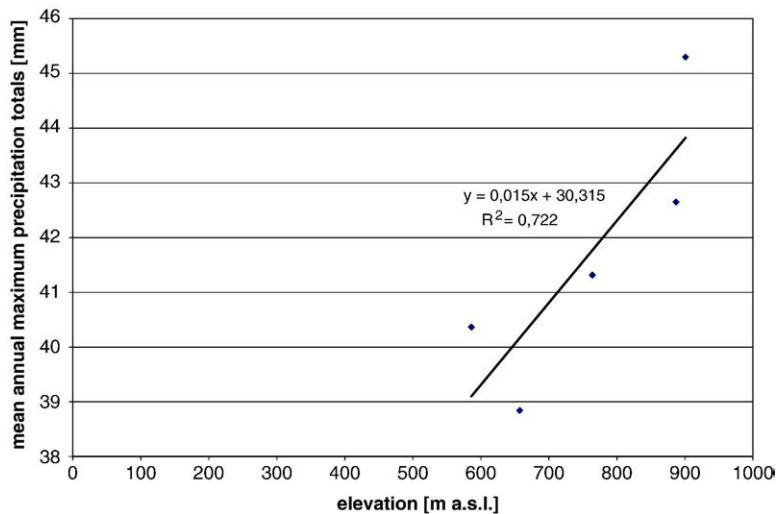


Fig. 10. Relationship of the mean annual maximum 24-hour precipitation with elevation for the sub-region No 1.

case of the occurrence of local extremes with a high degree of differences in their spatial distribution during convective atmospheric events.

From a comparison of the maps of 100-year maximum daily precipitation totals the similarity between mapping approaches A and B is obvious. In map C, the effect of the local extremes of the daily precipitation is again evident. Map D expresses the effect of the regional estimation; the pattern of leeward stations 5, 13, 15 and the pattern of windward stations 1, 10, 20, 21 and 23 can be seen.

A similarity between the IDW and kriging interpolations by mutual comparison of both methods was also observed. In Fig. 13a and b percentage differences in maps of the design annual maximum daily precipitation totals using the kriging interpolation method from the maps derived using the IDW interpolation are shown.

As it can be seen from the figures, both methods are rather similar. In the maps of 2-year maximum daily precipitation totals, differences for all the mapping approaches are in a range from -5 to $+5\%$ for almost the whole region. In the mapping approaches A, B and D only for a small area located in the south-western part of the region (with a sparse dataset) differences in a range from -5 to -10% were indicated. In the mapping approach C, differences from -5 to -10% were recognized in small areas around stations. In maps of 100-year maximum daily precipitation totals (Fig. 13b), the tendency of differences between both interpolation methods is the same. For mapping approaches A, B and D the south-western area with a sparse dataset with differences from -5 to -10% is larger than for 2-year design values. In method C, a stronger effect of local overestimation of design precipitation at the station sites by the IDW interpolation is indicated than for 2-year design values.

The predictive accuracy of the different approaches to mapping the design annual maximum daily precipitation totals was compared by the jackknife cross-validation error. This is a measure of the difference between the mapped value for a station, when the station has been removed from the data set, and the station's value. The error statistics of

jackknife cross-validation for different approaches to mapping design maximum daily precipitation totals are presented in Tables 6 and 7. The statistics include variation, standard deviation, average, median, minimum and maximum of errors in design annual maximum daily precipitation (in mm and %) over 23 precipitation stations.

Tables 6 and 7 show relatively consistent results for the different mapping approaches used, with certain distinctions between them. The IDW and kriging interpolations are very similar; some differences can be seen for the nearest neighbor interpolation method.

Variations and standard deviations of errors in the design annual maximum daily precipitation are rather similar for all the mapping approaches and interpolation methods. For the 2-year maximum daily precipitation totals, the variations of errors vary from 10.7 to 14.5 mm (44 to 71.8%), and the standard deviations vary from 3.3 to 3.8 mm (7.1 to 8.5%). For the 100-year maximum daily precipitation totals, the variations of errors are higher, in a range from 128 to 243 mm (122 to 283%), and the standard deviations of the errors are in a range from 11.3 to 15.6 mm (11 to 16.8%). The highest variations and standard deviations of errors in the design precipitation were achieved for the mapping method based on the interpolation of daily precipitation totals using the nearest neighbor interpolation method. Generally, the nearest neighbor interpolation method caused the highest variations and standard deviations of errors in all the mapping approaches.

The negative averages and medians of errors in the design annual maximum daily precipitation totals reveal an underestimation of these values for almost all the approaches, with a higher degree of underestimation for the method based on the interpolation of daily precipitation totals. For the 2-year maximum daily precipitation totals, averages of the errors change from -0.02 to 0.07 mm (0.4 to 0.6%) for the at-site and moments mapping approaches, from -0.99 to -0.92 mm (-1.8 to -1.6%) for the regional mapping approach, and from -5.9 to -5.4 mm (-12.7 to -11.7%) for the mapping approach based on the interpolation of the daily precipitation totals, using the inverse distance and kriging interpolations (but

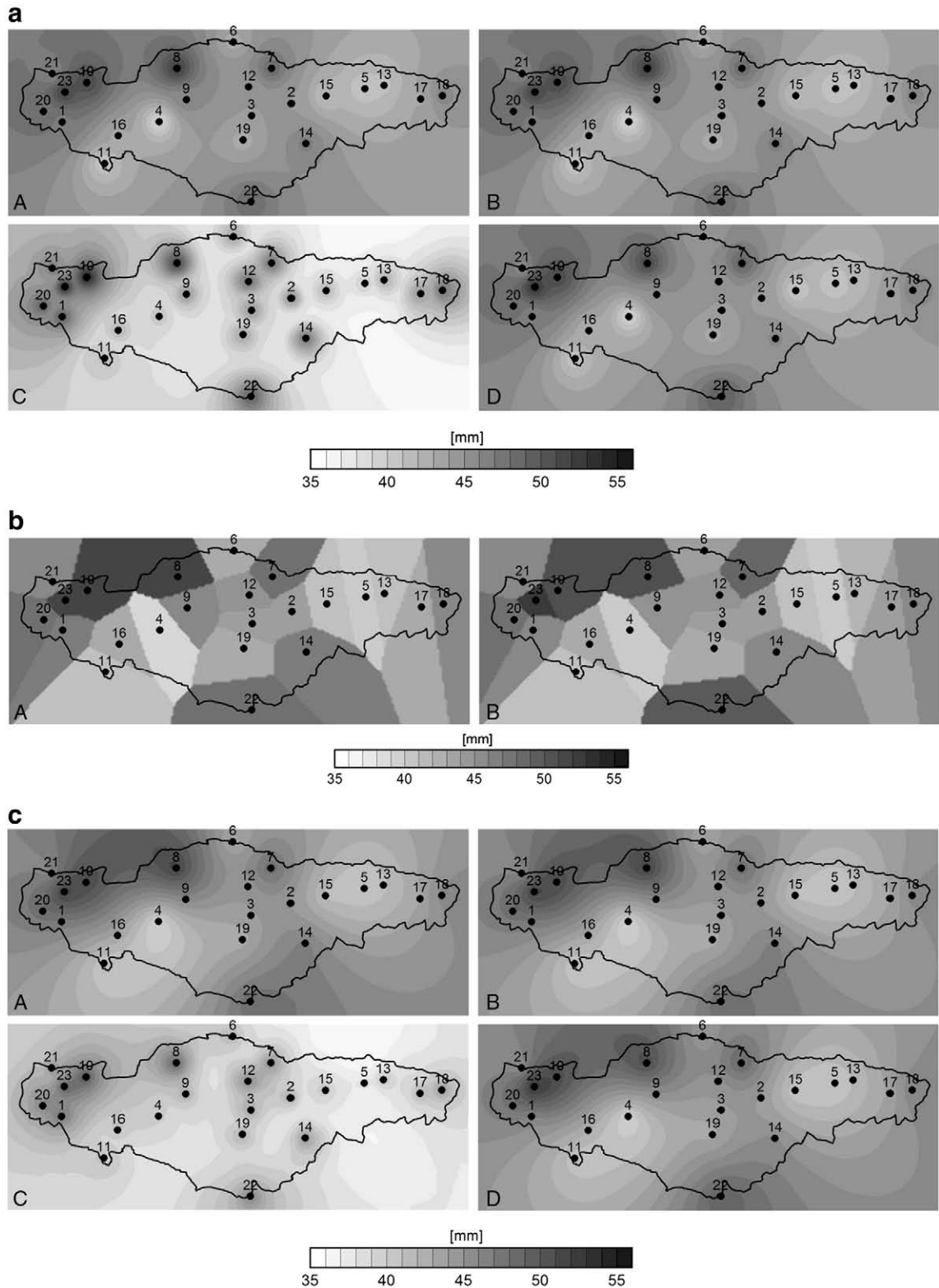


Fig. 11. a. Maps of 2-year maximum daily precipitation totals derived by different mapping approaches using IDW interpolation (A = at site, B = interpolation of GEV moments, C = interpolation of daily precipitation, D = regional interpolation). b. Maps of 2-year maximum daily precipitation totals derived by different mapping approaches using nearest neighbour interpolation (A = at site, interpolation of GEV moments and interpolation of daily precipitation, B = regional interpolation). c. Maps of 2-year maximum daily precipitation totals derived by different mapping approaches using kriging interpolation (A = at site, B = interpolation of GEV moments, C = interpolation of daily precipitation, D = regional interpolation).

only 0.3 mm, i.e. 0.5%, using the nearest neighbor interpolation). For the 100-year maximum daily precipitation totals, the averages of the errors change from -1.36 to -0.45 mm (-0.8 to 0.9%) for the at-site and moments mapping approaches, from -7.9 to -7.8 mm (-7.6 to -7.5%) for the regional mapping approach, and from -19.7 to -18.4 mm (-20.7 to -19.5%) for the mapping approach based on the interpolation of the daily precipitation totals, using the inverse distance and kriging interpolations (but only -0.8 mm, i.e. 0.3%, using the nearest neighbor interpolation).

Very similar results were obtained for the medians of the errors in the design annual maximum daily precipitation totals.

Some differences between the mapping approaches are evident in the minimum and maximum values of the errors in the design annual maximum daily precipitation totals. For the 2-year maximum daily precipitation totals, the minimum of the errors are in a range from -14 to -6 mm (-28 to -11%) and the maximum errors in a range from -4 to 6.7 mm (-1.2 to 17.5%). For the 100-year maximum daily precipitation totals, the minimum values of the errors range from -60 to -32 mm (-47 to -26%) and the maximum errors are in a range from 3.9 to 32.6 mm (5.2 to 35.1%).

The highest degree of underestimation in the averages and medians of the errors in the design annual maximum daily precipitation totals is apparent for the mapping method based on the interpolation of the daily precipitation totals. This fact follows from the disadvantage of the jackknife interpolation, which heavily smoothes and reduces the local extremes of the daily precipitations, particularly those that occur during summer convective atmospheric events.

In Figs. 14 and 15, the percentage errors between the design annual maximum daily precipitation totals from different mapping approaches and the at-site estimation analyzed by the jackknife cross-validation are expressed. Only the kriging interpolation method is illustrated here.

From the results in Figs. 14 and 15 similar behaviors with respect to over- and underestimation in the A, B and D methods can be seen, while the considerable underestimation of the design values for all stations for method C became obvious.

5. Discussion

The spatial pattern of precipitation is known to be highly dependent on meteorological conditions and topography in general. But the relationships between the annual maximum 24-hour precipitation and topography in the Hron region are not very well explainable by such general patterns, partly because of the mixture of scales involved in the data generation (local and synoptic scale events), and the low altitudinal zonality of the mapped variables and the complex topography which introduces a combination of only local orographic effects in the north-western and eastern part of the region. Other, more developed, regional patterns in the generation of precipitation were not discovered. This fact was also acknowledged by climatological experts; they therefore prefer the use of subjective knowledge based mapping of precipitation extremes (Gaál et al., 2004). Despite the fact that a reasonable number of gauges were available for the mapping, their spatial distribution was rather uneven, with high densities in lowland areas and much more

sparse coverage in high mountain ranges. The resulting scarcity of information available to study precipitation regimes in high elevation areas also contributed to the difficulties. Moreover, the gauges situated in the valleys may not be representative of the high mountainous areas in the case of frontal convective events. These facts dominated the rather random spatial patterns in the design precipitation distribution. As for the applicability of the tested mapping approaches under these conditions, the following has to be taken into consideration.

The first method, the direct mapping of quantiles, is based on local statistical estimates. Although here a unified frequency distribution was used, it does not have to be so in each practical case. Tail behavior of distribution functions differs, and the uncertainty of the quantile estimates may also differ at each station as a function of the length and quality of the at-site data and the distribution chosen. These facts would influence the final quality of the map of quantiles, which would then be built on statistically non-homogeneous information.

The second method, the direct mapping of the distribution function parameters, suffers from the same drawbacks; moreover, the choice of the unified distribution function which is required in this case could be done arbitrarily in practical case studies depending on the skills of the analyst or could be forced upon the data even in cases where such approach would not be possible. As a result, the map of parameters would then be again built on statistically non consistent and possibly erroneous information.

The third method based on interpolation of daily precipitation has a good deal of potential in principle, but only in cases when the conditions for such mapping of daily data are favorable. The major potential advantage of the proposed algorithm in comparison to the direct mapping of design precipitation values and distribution quantiles is that, given that physically adequate interpolation is used and adequate data is available, it enables the estimation of design values at ungauged sites for an interpolated time series which may better reflect the physical and regional properties of precipitation extremes, as well as a description of the seasonal variations of extreme daily precipitation totals over a selected region.

In the case of the upper Hron River basin, conditions for the successful application of the proposed method were not sufficiently met. That problem may have caused the underestimation of design precipitation even in the stations used for cross validation. It seems that the influence of small-scale thunderstorms caused by summer convection overrides the regularities which might be introduced by frontal convection (however, no event-based analysis was made in this case study in support of this statement). Due to the uneven spatial distribution of the raingauge network (despite of its mean network density of 77 km² per gauge in the catchment), this obviously does not fit into the scale, shapes and possibly also location of summer thunderstorms and in consequence it does not sufficiently describe these convective events.

Therefore this approach, despite its good potential, cannot be recommended as a basis for mapping in our case and also in similar cases. It would need to be complemented by other data sources, such as radar observations (e.g., Pegram, 2004) or supported by retrospective outputs from a local area meteorological model.

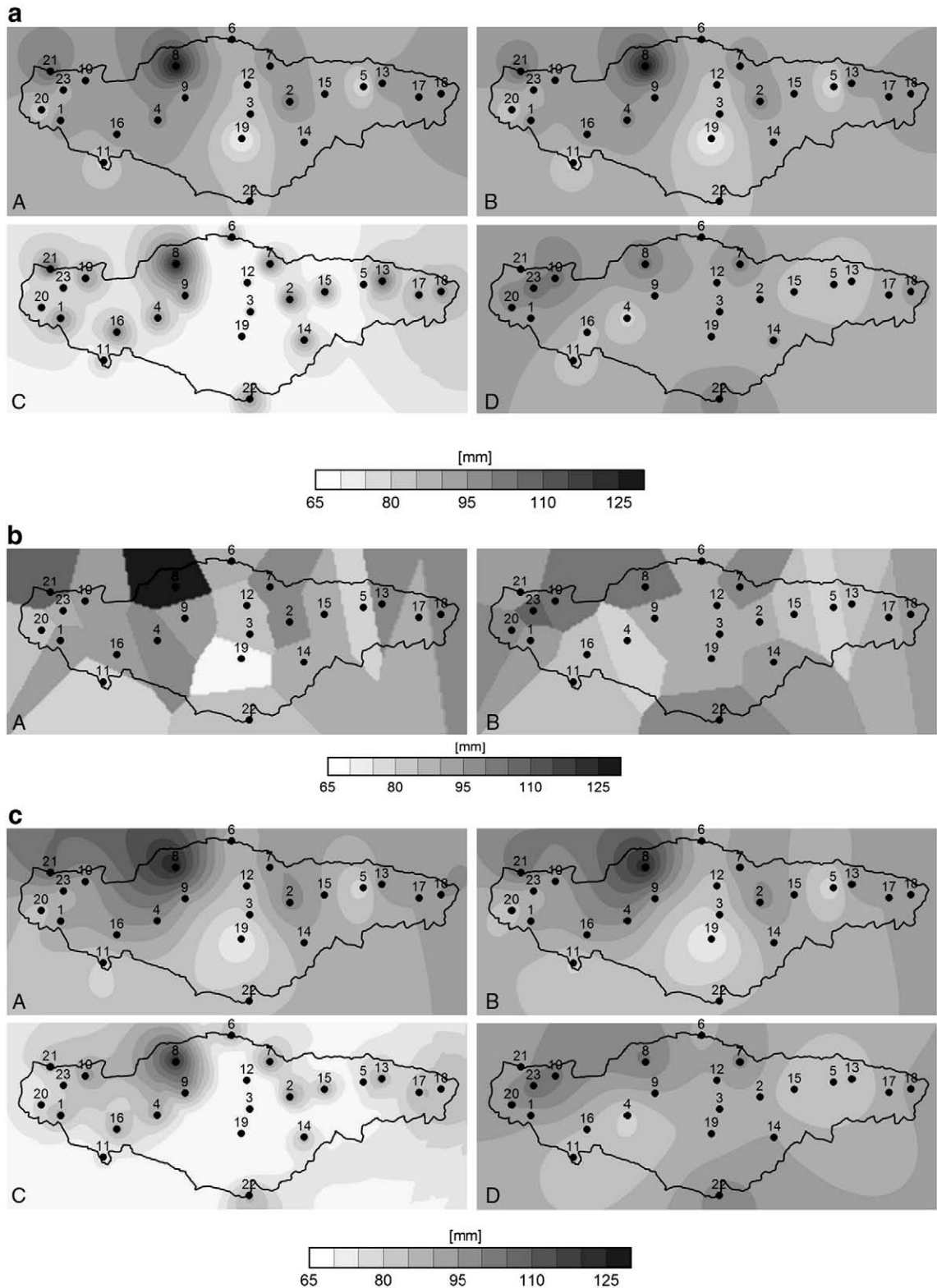


Fig. 12. a. Maps of 100-year maximum daily precipitation totals derived by different mapping approaches using IDW interpolation (A = at site, B = interpolation of GEV moments, C = interpolation of daily precipitation, D = regional estimation). b. Maps of 100-year maximum daily precipitation totals derived by different mapping approaches using nearest neighbour interpolation (A = at site, interpolation of GEV moments and interpolation of daily precipitation, B = regional interpolation). c. Maps of 100-year maximum daily precipitation totals derived by different mapping approaches using kriging interpolation (A = at site, B = interpolation of GEV moments, C = interpolation of daily precipitation, D = regional estimation).

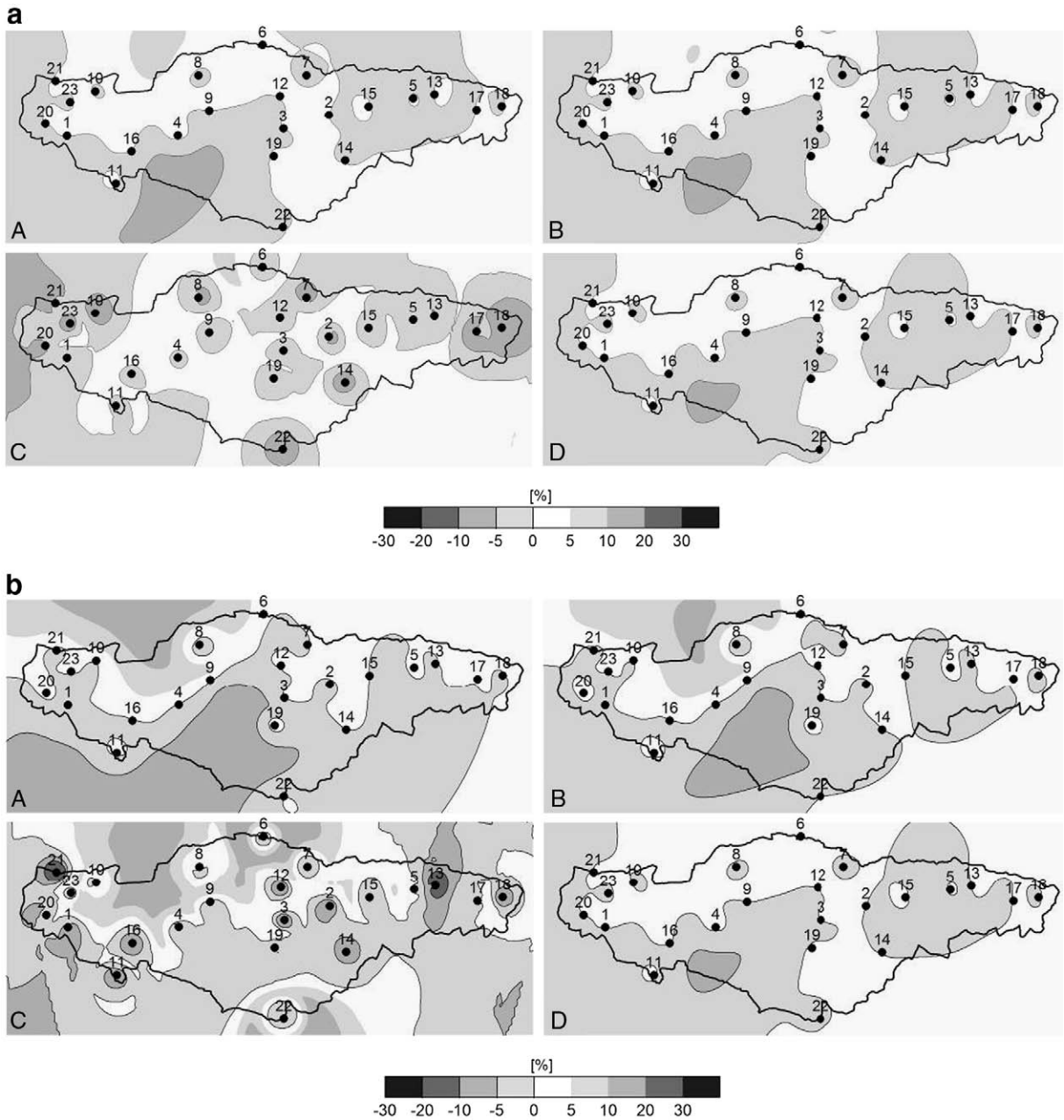


Fig. 13. a. Percentage differences in maps of 2-year maximum daily precipitation totals using the kriging interpolation method from maps derived using the IDW interpolation (A = at site, B = interpolation of GEV moments, C = interpolation of daily precipitation, D = regional interpolation). b. Percentage differences in maps of 100-year maximum daily precipitation totals using the kriging interpolation method from maps derived using the IDW interpolation (A = at site, B = interpolation of GEV moments, C = interpolation of daily precipitation, D = regional interpolation).

In the fourth method, the regional frequency analysis method, the patterns in the maps resulted mainly from the patterns generated from the mapping of the index value (the mean annual maximum 24-hour precipitation) and were influenced also by the special local conditions including the nonexistence of altitudinal variability of the parameters of the distribution function and the interpolation methods used.

From a statistical point of view, the spatial distribution of quantiles is theoretically better underpinned in the regional frequency approach than in the other methods tested. The method used here could be extended by regional regression for the index value in areas where terrain or other controls would contribute to an explanation of the spatial variability of this variable. A further refinement was suggested in Wallis et al. (2007), where the parameters of the distribution

Table 6

Error statistics of jackknife cross-validation for different mapping approaches to 2-year maximum daily precipitation totals ($n=23$ stations).

	Variation	Standard deviation	Average	Median	Min	Max
	(mm)	(mm)	(mm)	(mm)	(mm)	(mm)
at site_IDW	10.73	3.28	0.03	0.58	-7.24	6.73
at site_nn	12.01	3.47	0.06	0.41	-6.11	6.77
at site_kr	11.48	3.39	-0.02	0.25	-6.68	6.17
mom_IDW	10.72	3.27	0.04	0.59	-7.22	6.73
mom_nn	12.01	3.47	0.07	0.41	-6.11	6.77
mom_kr	10.98	3.31	-0.01	0.34	-6.74	6.18
int_IDW	12.84	3.58	-5.43	-4.26	-14.35	0.17
int_nn	14.50	3.81	0.03	-0.46	-6.11	6.77
int_kr	11.91	3.45	-5.85	-4.55	-14.74	-0.45
ieg_IDW	10.68	3.27	-0.95	-0.27	-8.27	5.43
reg_nn	12.97	3.60	-0.92	-0.52	-7.72	5.98
reg_kr	11.01	3.32	-0.99	-0.95	-7.79	4.66
	(%)	(%)	(%)	(%)	(%)	(%)
at site_IDW	53.2	7.3	0.6	1.3	-14.0	17.4
at site_nn	60.8	7.8	0.5	0.9	-11.8	17.5
at site_kr	56.6	7.5	0.4	0.6	-12.9	15.9
mom_IDW	53.5	7.3	0.6	1.3	-14.0	17.4
mom_nn	60.8	7.8	0.5	0.9	-11.8	17.5
mom_kr	54.2	7.4	0.4	0.8	-13.1	15.9
int_IDW	50.0	7.1	-11.7	-10.5	-27.8	0.4
int_nn	71.8	8.5	0.45	-1.0	-11.8	17.5
int_kr	44.61	6.7	-12.7	-11.2	-28.6	-1.2
reg_IDW	50.1	7.1	-1.6	-0.6	-16.0	14.0
reg_nn	62.7	7.9	-1.7	-1.2	-15.0	13.3
reg_kr	51.5	7.2	-1.8	-2.2	-15.1	12.0

at site – interpolation of design precipitation, mom – interpolation of GEV moments, int – interpolation of daily precipitation, reg – regional interpolation, IDW – inverse distance weighting, nn – nearest neighbour, kr – kriging.

function were regressed at the mean annual precipitation, which is usually easier to map. In the given case, however, none of these extensions were applicable due to the specific character of the dataset and the size of the region.

This method also has drawbacks, which are mainly based on the fact that despite fair theoretical foundations, a number of subjective decisions which have to be taken in the course of the analysis can result in the fact that the outcome of such a regional exercise is not unique and depends on the analyst's skills and preferences.

Despite such problems, regional frequency analysis has to be considered as a suitable candidate for preprocessing daily rainfall data for mapping of design precipitation in similar real-life applications as it is in the Hron case. Until sufficient quantitative information becomes available on the spatial distribution of the precipitation process with the desired spatial and temporal scales, by trading space for time, it overcomes the data shortage and problem of the unequal length of series through the expected and quantitatively underpinned spatial homogeneity principle. It also offers a solution to the problem of inadequate spatial coverage and sampling of precipitation fields by the gauging network.

As for the interpolation methods tested, the following has to be taken into consideration. Results from the nearest neighbor method are acceptable when considering cross validation; however this only gives information about the gauged sites. The spatial patterns introduced by this method

are, as expected, very simple and the method should be used only in the case of sparse data.

Despite the fact that usual mapping methods such as ordinary kriging and inverse distance are considered adequate only for simple climate patterns (Daly, 2006), here, their application was considered justified both by the properties of the data and the engineering scenario chosen. Both methods assume that the process which is modeled does not depend on the spatial location, and that the variance of the difference between two values depends only on the distance between the two points and not on the location. On the other hand this common feature caused that the results of both methods exhibit visually and numerically similar results.

6. Conclusions

The purpose of the study was to produce maps of 2-year and 100-year daily precipitation as extreme rainfall indexes which could be used in engineering hydrology for rainfall-runoff studies and estimating flood hazard. In follow up investigations the mapped information could be further processed by engineering hydrologic methods such as temporal disaggregation and/or the spatial reduction of the design precipitation values. The choice of data processing methods was guided not only by the analysis of the data but also by their practical applicability and acceptance in the engineering hydrologic community.

Table 7

Error statistics of jackknife cross-validation for different mapping approaches to 100-year maximum daily precipitation totals ($n=23$ stations).

	Variation	Standard deviation	Average	Median	Min	Max
	(mm)	(mm)	(mm)	(mm)	(mm)	(mm)
at site_IDW	145.71	12.07	-0.45	-0.08	-35.70	18.42
at site_nn	213.35	14.61	-1.23	-2.77	-32.58	25.60
at site_kr	153.56	12.39	-0.46	-1.69	-32.89	18.33
mom_IDW	143.38	11.97	-1.36	-1.39	-36.16	17.82
mom_nn	213.87	14.62	-1.27	-2.77	-32.58	26.28
mom_kr	143.09	11.96	-1.04	-2.58	-33.31	18.14
int_IDW	188.48	13.73	-19.65	-20.08	-60.08	8.34
int_nn	243.08	15.59	-0.77	-2.77	-32.58	32.58
int_kr	193.54	13.91	-18.43	-18.10	-56.49	3.92
reg_IDW	129.33	11.37	-7.83	-8.10	-44.13	13.08
reg_nn	138.04	11.75	-7.79	-5.58	-43.10	11.70
reg_kr	128.86	11.35	-7.91	-8.56	-43.22	13.17
	(%)	(%)	(%)	(%)	(%)	(%)
at site_IDW	164.2	12.8	0.9	-0.1	-28.5	26.9
at site_nn	249.1	15.8	-0.2	-2.9	-26.0	27.6
at site_kr	173.9	13.2	-0.8	-1.9	-26.2	24.4
mom_IDW	160.7	12.7	0.6	-1.6	-28.8	25.9
mom_nn	249.7	15.8	0.5	-2.9	-26.0	28.3
mom_kr	161.8	12.7	0.4	-2.9	-26.5	24.1
int_IDW	158.0	12.6	-20.7	-22.8	-47.9	11.1
int_nn	283.8	16.8	0.3	-2.9	-26.0	35.1
int_kr	169.9	13.0	-19.5	-19.4	-45.0	5.2
reg_IDW	122.0	11.0	-7.5	-9.2	-35.2	19.1
reg_nn	130.2	11.4	-7.5	-6.2	-34.3	17.1
reg_kr	123.7	11.1	-7.6	-9.7	-34.4	19.2

at site – interpolation of design precipitation, mom – interpolation of GEV moments, int – interpolation of daily precipitation, reg – regional interpolation, IDW – inverse distance weighting, nn – nearest neighbour, kr – kriging.

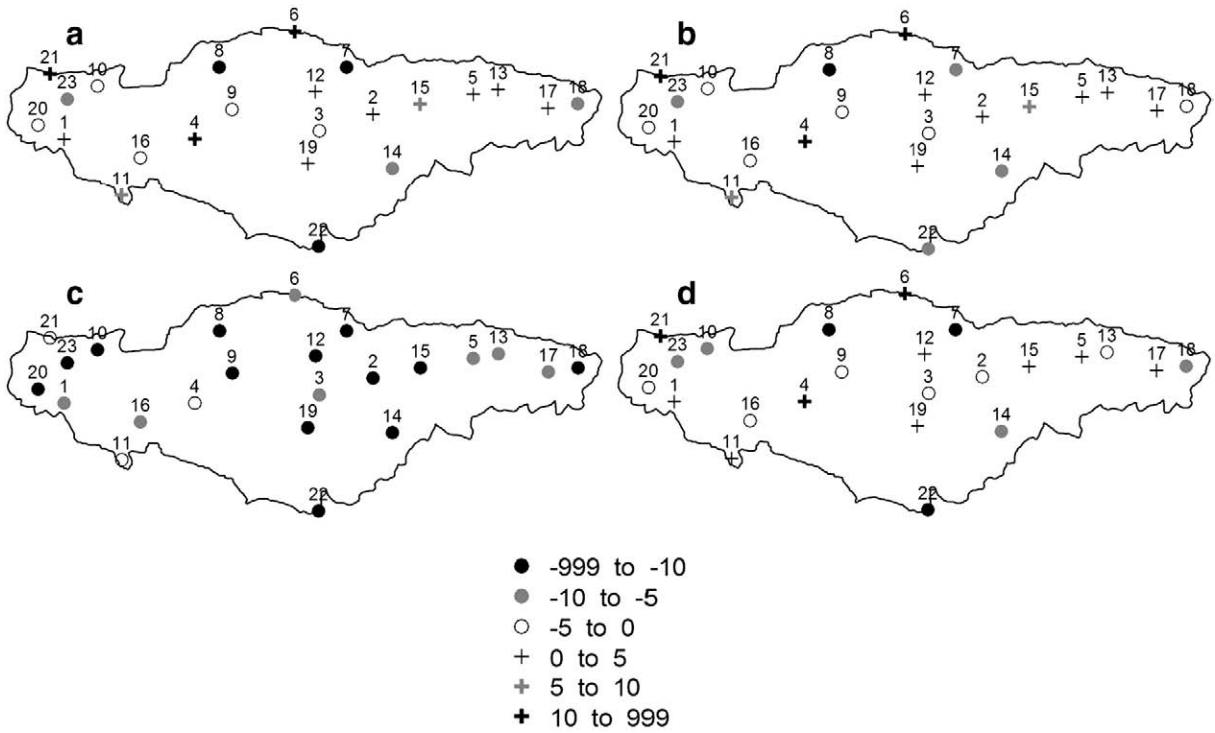


Fig. 14. Percentage errors of 2-year maximum daily precipitation totals from the jack-knife cross-validation for different mapping approaches and kriging interpolation (a = at site, b = moments interpolation, c = interpolation of daily precipitation, d = regional estimation).

Four approaches to the preprocessing of data to be mapped were used and three interpolation methods employed. Combinations of the respective results were described and

compared with a special emphasis on the spatial patterns introduced by each processing and mapping approach to the final maps. The study was not aimed at finding the best

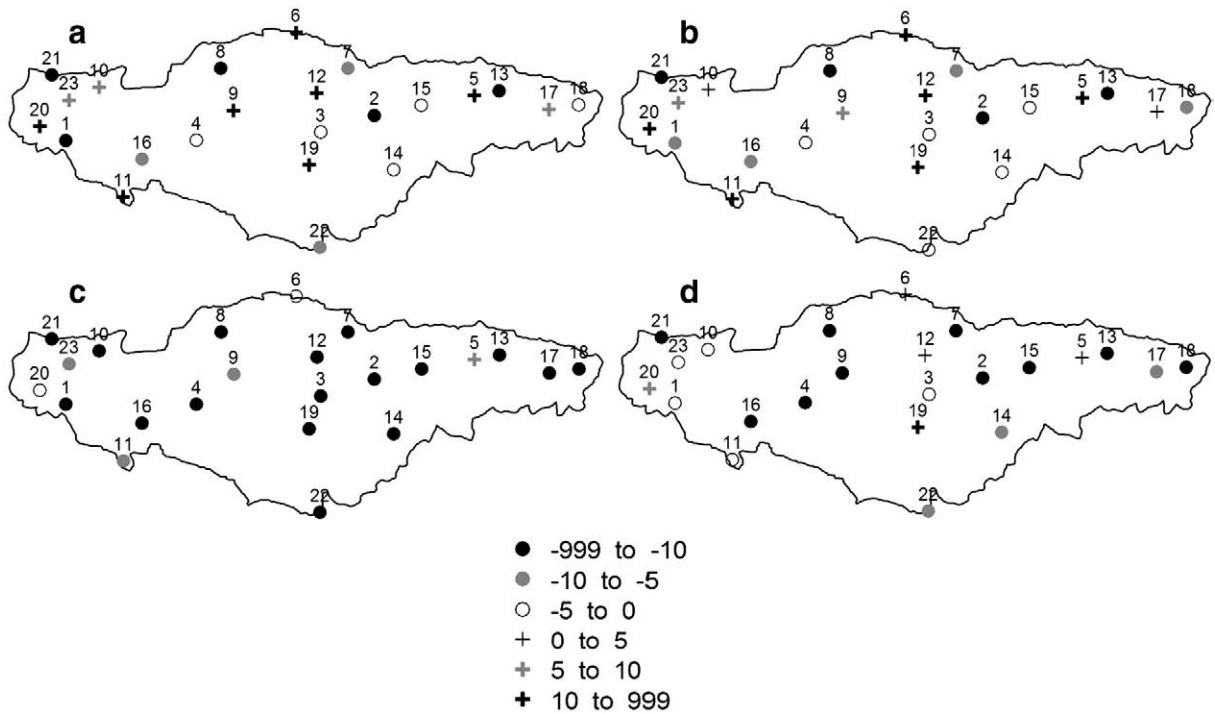


Fig. 15. Percentage errors of 100-year maximum daily precipitation totals from the jack-knife cross-validation for different mapping approaches and kriging interpolation (a = at site, b = moments interpolation, c = interpolation of daily precipitation, d = regional estimation).

method; it was intended more to comment on the quality and properties of the final products (maps of design precipitation with a given return period) with respect to the expectations of the end user community.

Daly (2006) suggests that complex regions, such as those that have significant terrain features and also significant coastal effects, rain shadows, or cold air drainage and inversions, are best handled by sophisticated systems that are configured and evaluated by experienced climatologists. That might well also be the case for the upper Hron basin, where in addition to the synoptic spatial scale, both Mediterranean and continental effects mix their influence. However such a complex approach can hardly be taken into consideration in engineering projects.

Two solutions can be suggested for such conditions, in principle. One is to initiate and conduct countrywide studies of mapping extremes (such as that described in Wallis et al., 2007) supported by extensive background data and knowledge. In small scale studies the use of one of the available versions of the regional frequency approach could be recommended as a suitable method to account for spatial variability. It is well described in the literature and supported by appropriate software. The drawbacks of the approach lie in the problem of solving discontinuities on the borders of regions (which were avoided here by the suggestion that the whole region be taken as homogeneous area) and in subjective decisions which are to be taken when delineating regions, which require a high degree of skill from the analysts.

As the second, regional frequency analysis can be considered as a suitable candidate for preprocessing daily rainfall data for mapping of design precipitation in similar real-life applications as it is in the Hron case. By trading space for time it overcomes the data shortage problem, and through the expected and quantitatively underpinned spatial homogeneity, it also offers a solution to the problem of inadequate spatial coverage and sampling of the precipitation fields by the gauging network.

For the future in practice, until radar-based times series will become long enough to be considered in statistical analysis, meteorological re-analysis focused on the synoptic background conditions for heavy, localised rainfall events could also be considered as a solution. These would be diagnosed through the joint analysis of surface precipitation and re-analysis of large-scale atmospheric fields as well as the design of composite maps conditioned on the occurrence of events within local regions. The retrospective use of LAMS could also support such studies. However, for engineering projects, such undertakings may probably stay to be too complicated; therefore, the use of regional frequency analysis can be seen as an adequate substitute.

Acknowledgement

This work was supported by the European Community's Sixth Framework Programme through the grant to the budget of the STREP Project *HYDRATE*, Contract GOCE 037024. The authors also gratefully acknowledge the VEGA grant agency for the support of grants 1/4024/07 and 1/0496/08.

References

Ahrens, B., 2006. Distance in spatial interpolation of daily rain gauge data. *Hydrol. Earth Syst. Sci.* 10, 197–208.

- Asli, M., Marcotte, D., 1995. Comparison of approaches to spatial estimation in a bivariate contest. *Math. Geol.* 27, 641–658.
- Barthels, H., Malitz, G., Asmus, S., Albrecht, F.M., Dietzer, B., Günther, T., Ertel, H., 1997. Starkniederschlagshöhen für Deutschland, KOSTRA. Deutscher Wetterdienst, Hydrometeorologie, Offenbach, Selbstverlag.
- Beguieria, S., Vicente-Serrano, S.M., 2006. Mapping the hazard of extreme rainfall by peaks over threshold extreme value analysis and spatial regression techniques. *J. Appl. Meteorol. Climatol.* 45, 108–124.
- Bloeschl, G., Grayson, R., 2001. Spatial observations and interpolation. In: Grayson, R., Bloeschl, G. (Eds.), *Spatial Patterns in Catchment Hydrology: Observation and Modeling*. Cambridge University Press, UK. ISBN: 0-521-63316-8, 17–50.
- Bonnin, G.M., 2003. Recent updates to NOAA/NWS rainfall frequency atlases. *World Water and Environmental Resources Congress*, pp. 1681–1690.
- Borga, M., Vizzacaro, A., 1997. On interpolation of hydrologic variables: formal equivalence of multiquadratic surface fitting and kriging. *J. Hydrol.* 195 (1–4), 160–171.
- Brown, D.P., Comrie, A.C., 2002. Spatial modeling of winter temperature and precipitation in Arizona and New Mexico, USA. *Clim. Res.* 22, 115–128.
- Burn, D.H., 1990. Evaluation of regional flood frequency analysis with a region of influence approach. *Water Resour. Res.* 26 (10), 2257–2265.
- Burn, D.H., 1997. Catchment similarity for regional flood frequency analysis using seasonality measures. *J. Hydrol.* 192 (1–4), 212–230.
- Casas, C.M., Herrero, M., Ninyerola, M., Pons, X., Rodriguez, R., Riusb, A., Redanoe, A., 2007. Analysis and objective mapping of extreme daily rainfall in Catalonia. *Int. J. Climatol.* 27, 399–409.
- Carrera-Hernández, J.J., Gaskin, S.J., 2007. Spatio temporal analysis of daily precipitation and temperature in the Basin of Mexico. *J. Hydrol.* 336, 231–249.
- Cipra, T., 1986. *Time Series Analysis with Application in Economy* (in Slovak). SNTL, Praha, Czech Republic. 243 pp.
- Cooley, D., Nychka, D. and Naveau, P., 2007. Bayesian spatial modeling of extreme precipitation return levels. *J. Am. Stat. Assoc.* 102, 824–840.
- Cressman, G.P., 1959. An operational objective analysis system. *Mon. Weather Rev.* 87, 367–374.
- Cunnane, C., 1985. Factors affecting choice of distribution for flood series. *Hydrol. Sci. J.* 30 (1), 25–36.
- Dalrymple, T., 1960. Flood frequency methods. *U. S. Geol. Surv.* 1543-A, 11–51.
- Daly, Ch., 2006. Guidelines for assessing the suitability of spatial climate data sets. *Int. J. Climatol.* 26, 707–721.
- Dubois, G., 1998. Spatial interpolation comparison 97: foreword and introduction. *J. Geogr. Inf. Decis. Anal.* 2, 1–10.
- Faško, P., Lapin, M., Št'astný, P., Vivoda, J., 2000. Maximum daily sums of precipitation in Slovakia in the second half of the 20th century. *Images of Weather and Climate. Prace Geograficne, fasc., vol.108*. Institute of Geography of the Jagellonian University, Cracow, 131–138.
- Faulkner, D.S., Prudhomme, C., 1998. Mapping an index of extreme rainfall across the UK. *HESS* 2 (2–3), 183–194.
- FEH (Flood estimation handbook), 1999. Institute of Hydrology, Wallingford. vol. 1–5., 325 pp.
- Ferrari, E., 1994. Regional rainfall and flood frequency analysis in Italy. International Conference "Development in Hydrology of Mountainous Areas", Stará Lesná, Slovakia, 12–16 September 1994, 45–52.
- Flood studies report, 1975. Natural Environment Research Council.
- Gaál, L., 2006. Methods for estimation of statistical characteristics of design K-days precipitation totals in Slovakia (in Slovak), PhD. Thesis, Comenius University Bratislava, Slovakia, 227 pp. (in Slovak).
- Gaál, L., Lapin, M., Faško, P., 2004. Maximum several-day precipitation totals in Slovakia. In: Rožnovský, J., Litschman, T. (Eds.), *Extremes of Weather and Climate*. Brno.
- García-Ruiz, J.M., Arnáez, S.M., White, S.M., Lorente, A., Begeuería, 2000. Uncertainty assessment in the prediction of extreme rainfall events: an example from the central Spanish Pyrenees. *Hydrol. Process.* 14, 887–898.
- Geiger, H., Stehli, A., Castellazzi, U., 1986. Regionalisierung der Starkniederschläge und Ermittlung typischer Niederschlagsganglinien. *Beitr. Geol. Schweiz, Hydrol.* 33, 141–193.
- Goovaerts, P., 2000. Geostatistical approaches for incorporating elevation into the spatial interpolation of rainfall. *J. Hydrol.* 228, 113–129.
- Gottschalk, L., Krasovskaia, I., 2002. L-moment estimation using annual maximum (AM) and peak over threshold (POT) series in regional analysis of flood frequencies. *Nor. Geogr. Tidskr. – Nor. J. Geogr.* 56 (2), 179–187.
- HAD, Hydrologischer Atlas von Deutschland, 2003. Bundesministerium fuer Umwelt, Naturschutz und Reaktorsicherheit, Freiburger Verlagsgesellschaft.
- HADES, Hydrologischer Atlas der Schweiz, 2004. Bern.
- HAÖ, Hydrologischer Atlas Österreichs, 2003. Bundesministerium für Land- und Forstwirtschaft, Umwelt und Wasserwirtschaft, Österreichischer Kunst- und Kulturverlag, Wien.
- Hlavčová, K., Kohnová, S., Kubeš, R., Szolgay, J., Zvolenský, M., 2005. An empirical method for estimating future flood risk for flood warnings. *Hydrol. Earth Syst. Sci.* 9 (4), 431–488.

- Hofierka, J., Parajka, J., Mitášová, H., Mitáš, L., 2002. Multivariate interpolation of precipitation using regularized spline with tension. *Trans. GIS* 6 (2), 135–150.
- Hosking, J.R.M., 1990. L-moments: analysis and estimation of distributions using linear combinations of order statistics. *J. R. Stat. Soc., Ser. B* 52 (1), 105–124.
- Hosking, J.R.M., Wallis, J.R., 1993. Some statistics useful in regional frequency analysis. *Water Resour. Res.* 29 (2), 271–281.
- Hosking, J.R.M., Wallis, J.R., 1997. *Regional Frequency Analysis*. Cambridge University Press, Cambridge, UK.
- Isaaks, E.H., Srivastava, R.M., 1989. *An Introduction to Applied Geostatistics*. Oxford University Press, New York. 561 pp.
- Jarvis, C.H., Stuart, N., 2001. A comparison among strategies for interpolating maximum and minimum daily air temperatures. Part II. The interaction between number of guiding variables and the type of interpolating method. *J. Appl. Meteorol.* 40, 1075–1084.
- Katz, R.W., Parlange, M.B., Naveau, Ph., 2002. Statistics of extremes in hydrology. *Adv. Water Resour. Elsevier* 25, 1287–1304.
- Kite, G.W., 1977. *Frequency and risk analysis in hydrology*. Water Resources Publications, Fort Collins, Colorado.
- Landscape Atlas of the Slovak Republic, 2002. Slovak Agency for the Environment, Banská Bystrica.
- Lang, H., Grebner, D., Kovar, K., Tappeiner, U., Peters, N.E., Craig, R.G., 1998. On large-scale topographic control of the spatial distribution of extreme precipitation and floods in high mountain regions. *Hydrology, Water Resources and Ecology in Headwaters*. IAHS Press, Wallingford, 47–50. IAHS No. 248.
- Lapin, M., Št'astný, P., Faško, P., Gaál, L., 2002. Project VTP 27-34, E 04 01: analysis of flood system in the upper Hron region. *Analysis of Climate – Hydrological Part (in Slovak)*, 54 pp.
- Lloyd, C.D., 2005. Assessing the effect of integrating elevation data into the estimation of monthly precipitation in Great Britain. *J. Hydrol.* 308, 128–150.
- Loukas, A., Vasiliades, L., Dalezios, N.R., Domenikiotis, C., 2001. Rainfall-frequency mapping for Greece. *Phys. Chem. Earth, Part B* 26/9, 669–674.
- Malitz, G., 2005. *Grundlagenbericht über Starkniederschlagshöhen in Deutschland, (Grundlagenbericht KOSTRA-DWD-2000)*. Deutscher Wetterdienst – Hydrometeorologie.
- Meijerink, A.M.J., De Brower, H.A.M., Manaert, C.M., Valenzuela, C.R., 1994. *Introduction to the Use of Geographic Information Systems for Practical Hydrology*. ITC publication no. 23, The Netherlands.
- Mitášová, H., Mitáš, L., 1993. Interpolation by regularized spline with tension: I. Theory and implementation. *Math. Geol.* 25, 41–655.
- Parajka, J., Kohnová, S., Szolgay, J., 2002. Spatial interpolation of maximum daily precipitation totals in the upper Hron region. *Acta Hydrol. Slovaca* 3/1, 35–45 (in Slovak).
- Parajka, J., Kohnová, S., Szolgay, J., 2004. Mapping the maximum daily precipitation totals in the upper Hron region using stochastic interpolation methods. *Acta Hydrol. Slovaca* 5/1, 78–87 (in Slovak).
- Park, J.S., Jung, H.S., Kim, R.S., Oh, J.H., 2001. Modelling summer extreme rainfall over the Korean peninsula using Wakeby distribution. *Int. J. Climatol.* 21 (11), 1371–1384.
- Pecušová, Z., Holko, L., Parajka, J., Kostka, Z., 2004. Interpolation of daily precipitation in the upper Hron basin using kriging with external drift. *Acta Hydrol. Slovaca (ISSN1335-6291)* 1, 3–13 (in Slovak).
- Pegram, G.G.S., 2004. *Spatial interpolation and mapping of rainfall (SIMAR) Volume 3: Data Merging for Rainfall Map Production*, Report WRC 1153/1/04, Water Research Commission, Pretoria, South Africa, available on request for a nominal mailing fee.
- Pekárová, P., Pekár, J., 2004. Teleconnections of AO, NAO, SO and QBO with interannual streamflow fluctuation in the Hron basin. *J. Hydrol. Hydromech.* 52 (4), 279–290 ISSN 0042/790X.
- Pilgrim, D.H. (Ed.), 1987. *Australian Rainfall and Runoff. A Guide to Flood Estimation*. Institute of Engineers, Australia, vol. 1.
- Prudhomme, C., 1999. Mapping a statistic of extreme rainfall in a mountainous region. *Phys. Chem. Earth, Part E* 24/1-2, 79–84.
- Reed, D.W., Faulkner, D.S., Stewart, E.J., 1999. The FORGEX method of rainfall growth estimation II: description. *Hydrol. Earth Syst. Sci.* 3, 197–203.
- Stalman, V., Draschoff, R., Günther, T., Pfister, A., Prellberg, D., Verworn, H.-R., Malitz, G., 2004. *Das Niederschlagsregelwerk für die deutsche Wasserwirtschaft*. Wasserwirtschaft 10, 8–27.
- Stedinger, J.R., 1983. Estimating a regional flood frequency distribution. *Water Resour. Res.* 19 (2), 503–510.
- Šamaj, F., Valovič, Š., Brázdil, R., 1985. Denné úhrny zrážok s mimoriadnou výdatnosťou v ČSSR v období 1901–1980. [Daily high-intensity rainfall in ČSSR during the period 1901 to 1980] *Works of SHMÚ 24. Alfa*, Bratislava, pp. 9–113 (in Slovak).
- Thiessen, A.H., 1911. Precipitation averages for large areas. *Mon. Weather Rev.* 39 (7), 1082–1084.
- Tabios, G.Q., Salas, J.D., 1985. A comparative analysis of techniques for spatial interpolation of precipitation. *Water Resour. Bull.* 21 (3), 365–380.
- Thompson, C.S., 1992. *HIRDS: Manual and Software*. National Institute of Water and Atmospheric Research Wellington.
- Thompson, C.S., 2002. The high intensity rainfall design system HIRD. In: Speafico, M. (Ed.), *International Conference on Flood Estimation*. CHR Report, No. II-17, International Commission of the Rhine Basin, Lelystad, 273–281.
- Vogel, R.M., Fenessey, N.M., 1993. L-moments diagrams should replace product moment diagrams. *Water Resour. Res.* 29 (6), 1745–1752.
- Wallis, J.R., Schaefer, M.G., Barker, B.L., Taylor, G.H., 2007. Regional precipitation–frequency analysis and spatial mapping for 24-hour and 2-hour durations for Washington State. *Hydrol. Earth Syst. Sci.* 11 (1), 415–442.
- Watkins Jr., D.W., Link, G.A., Johnson, D., 2005. Mapping regional precipitation intensity duration frequency estimates. *J. Am. Water Res. Assoc.* 41 (1), 157–170.
- Weisse, A.K., Bois, P., 2001. Topographic effects on statistical characteristics of heavy rainfall and mapping in the French Alps. *J. Appl. Meteorol.* 40 (4), 720–740.
- Weisse, A.K., Bois, P., 2002. A comparison of methods for mapping statistical characteristics of heavy rainfall in the French Alps: the use of daily information. *Hydrol. Sci. J.* 47 (5), 739–752.
- Wolfson, N., 1975. Topographical effects on standard normals of rainfall over Israel. *Weather* 30, 138–144.
- Wotling, G., Bouvier, C., Danloux, J., Fritsch, J.-M., 2000. Regionalization of extreme precipitation distribution using the principal components of the topographic environment. *J. Hydrol.* 233, 86–101.